ENERGY PERFORMANCE TESTING ON RECOVERY VENTILATORS AND DEVELOPMENT OF HRV/ERV TESTING FACILITY AS PER C439 STANDARD

A Thesis

by

ADITHYA SURESH ATHREYA

Submitted to the Office of Graduate and Professional Studies of
Texas A&M University
in partial fulfillment of the requirements for the degree of
MASTER OF SCIENCE

Chair of Committee,	Michael Pate
Committee Members,	Hong Liang
	Pavel Tsvetkov
Head of Department,	Bryan Rasmussen

December 2020

Major Subject: Mechanical Engineering

ABSTRACT

Heat recovery ventilators (HRVs), which is the focus of this research, transfer heat between two air streams, flowing in opposite directions, with one stream originating from the outdoors and other from a conditioned building space. The heating and cooling requirements in a conditioned space, (i.e., thermal zone) decrease as the outside air entering the HRV exchanges thermal energy with the exhaust air coming out of the thermal zone by bringing the outside air's temperature close to conditions necessary for human comfort. Even though HRV's are an important technology for reducing energy, there is a shortage of testing procedures and standards to ensure that units are designed and built for optimum performance.

Therefore, a central part of the research effort reported herein is the design and construction of an HRV testing facility at Texas A&M in the RELLIS Energy Efficiency Laboratory (REEL), College Station, Texas. The testing facility is a modification of the current standard used for the Home Ventilating Institute (HVI) certification of ventilators based on the CAN/CSA C439[1], Standard Laboratory Methods of Testing for Rating the Performance of Heat/Energy – Recovery ventilators. It should be noted that the design of the testing facility incorporates some aspects of the existing test methods. The reason for the modification is that one of the project's objective was to develop a more straightforward and faster test procedure applicable to hotter climates than what appears to be the general focus of the current cold-weather certification standard used by HVI.

The Energy performance of a typical residential HRV, namely a Fantech SHR200, was measured, analyzed, and evaluated by installing and operating it in this new testing facility. After performing extensive testing and creating a large database, the resulting Sensible Heat Recovery Efficiency

[1] Refer to CSA-C439 Standard Laboratory Methods of Test for Rating the Performance of Heat/Energy – Recovery Ventilators

(SHRE) and Effectiveness were found to be 32% and 58%, respectively, at the HRV's rated speed of 195 CFM. Upon further evaluation, it was found that the effectiveness and SHRE increases when the volumetric flow rate rises. The slope of rise is highest from 85 CFM to 155 CFM while the performance parameters show a modest rise from 155 CFM to 235 CFM. In addition to the energy performance study, error analysis, and airflow and thermal performance of the HRV were analyzed.

DEDICATION

I want to dedicate this thesis to my parents, who supported my educational endeavors and encouraged me to pursue higher studies after my undergrad. I want to thank my friends, who played defining roles in my life and, most importantly, kept me cheerful and optimistic.

I am grateful to them and cannot express my gratitude in simple words. I am always motivated by my family and friends to pursue challenges that I assumed were out of scope.

ACKNOWLEDGMENTS

I would like to thank Dr. Pate for mentoring me and providing guidance in my thesis. I am also thankful for the opportunity to work at REEL while being funded for my education. I want to thank Dr. Tsvetkov and Dr. Liang for accepting my request to play crucial roles as committee members and reviewing my thesis. I want to thank Dr. Sweeney for his guidance on management and work ethics in the industry.

I want to thank Troy Anora for his continuous support. I am grateful for having him as my project peer.

CONTRIBUTORS AND FUNDING SOURCES

CONTRIBUTORS

This work was supervised by a thesis committee consisting of Dr. Pate (Thesis Advisor) and Dr. Liang (Committee member) of the Department of Mechanical Engineering and Dr. Tsvetkov (Committee member) of the Department of Nuclear Engineering.

FUNDING

An assistantship supported my tuition and fees that was funded by Dr. Pate and the Energy Systems Laboratory.

NOMENCLATURE

HVI	Home Ventilating Institute
ANSI	American National Standards Institute
AMCA	Air Movement and Control Association International
ASHRAE	American Society of Heating, Refrigerating, and Air-Conditioning Engineers.
PHI	The Passive House Institute
HRV	Heat Recovery Ventilators
ERV	Energy Recovery Ventilators
CFM	Cubic Feet per Minute
SHRE	Sensible Heat Recovery Efficiency
REEL	RELLIS Energy Efficiency Lab
NECB	National Energy Code for Buildings
NBC	National Building Code

TABLE OF CONTENTS

Page

LIST OF FIGURES

Page

LIST OF TABLES

Page

1. INTRODUCTION

The primary goal of this project is to create a standard testing facility that can be used to certify and rate Heat Recovery and Energy Recovery ventilators (HRVs) following procedures and guidelines dictated by the governing body called the Home Ventilating Institute (HVI). There appear to be only two labs in North America, including REEL, that either test or are in the process of developing a facility to perform HVI testing of recovery ventilation units. Even then, these two labs have a major difference in that one focuses on cold-weather application, while the facility developed here focuses on the more moderate to hot climates.

This project opens a new arena for REEL to engage in HVI testing and certification and related research activities, which is essential since HRVs and ERVs are part of the Passive House Institute's (PHI) equipment testing and verification program. Furthermore, ASHRAE and LEED suggest that extra measures be taken to curb energy use in buildings and, especially HVAC systems, which utilize electricity, whose production contributes greatly to carbon emissions in the environment. With many Architectural and Engineering firms adopting HRV and ERV technology put forward by LEED and ASHRAE guidelines, many units and models will have to be certified for approval in future commercial and residential spaces.

A significant driver in the increased usage of HRVs and ERVs are the mandates that require meeting passive house quality. For a building to be called a Passive Building, six principles must be followed, namely: (1) high-performance insulation, (2) thermal bridge elimination, (3) optimal glazing, (4) shading, (5) airtightness, and (6) energy recovery ventilation implementations.

The sixth point is a driver because HRV and ERV technology is essential to minimize space thermal conditioning while maintaining a continuous flow of fresh air into the building. Presently, most homes rely on natural ventilation in the form of cracks in windows and doors, seals, and other openings throughout a dwelling. However, there are numerous drawbacks to natural ventilation, including unwanted drafts and high conditioning energy consumption due to the uncontrollability of airflow. If attempts are made to reduce this energy consumption by making buildings tighter, health, and Indoor Air Quality (IAQ) issues arise.

The main objective of ventilation units is to exchange, distribute, circulate, and treat air. Building performance should meet ASHRAE standards for IAQ and ventilation rates, as stated by the National Building Code (NBC), which have been adopted by many states in the US. The HVI organization has introduced principles and guidelines for testing and certifying HRV and ERV units to ensure that the unit's performances pass the CAN/CSA C439 standard's minimum criteria to fulfill the above objectives. There is significant agreement that this existing standard was developed for applications to cold-climate equipment where frosting is paramount, which means that testing of HRV and ERV units are a long and complicated process. In this regard, a new HRV/ERV testing facility applicable to warm and hot climates has been developed at Texas A&M University's RELLIS Energy Efficiency Lab (REEL) in College Station, Texas, to provide an alternative HVI accreditation approach to certify and test ventilation units for energy performance. This approach is not only more relevant to moderate to warm-weather climates but also easier and quicker to accomplish.

2. TESTING FACILITY DESIGN

2.1. FACILITY DESCRIPTION

The 3D model was essential for understanding how the testing facility should look when fully assembled, which also allowed for modifications to be implemented before the REEL testing

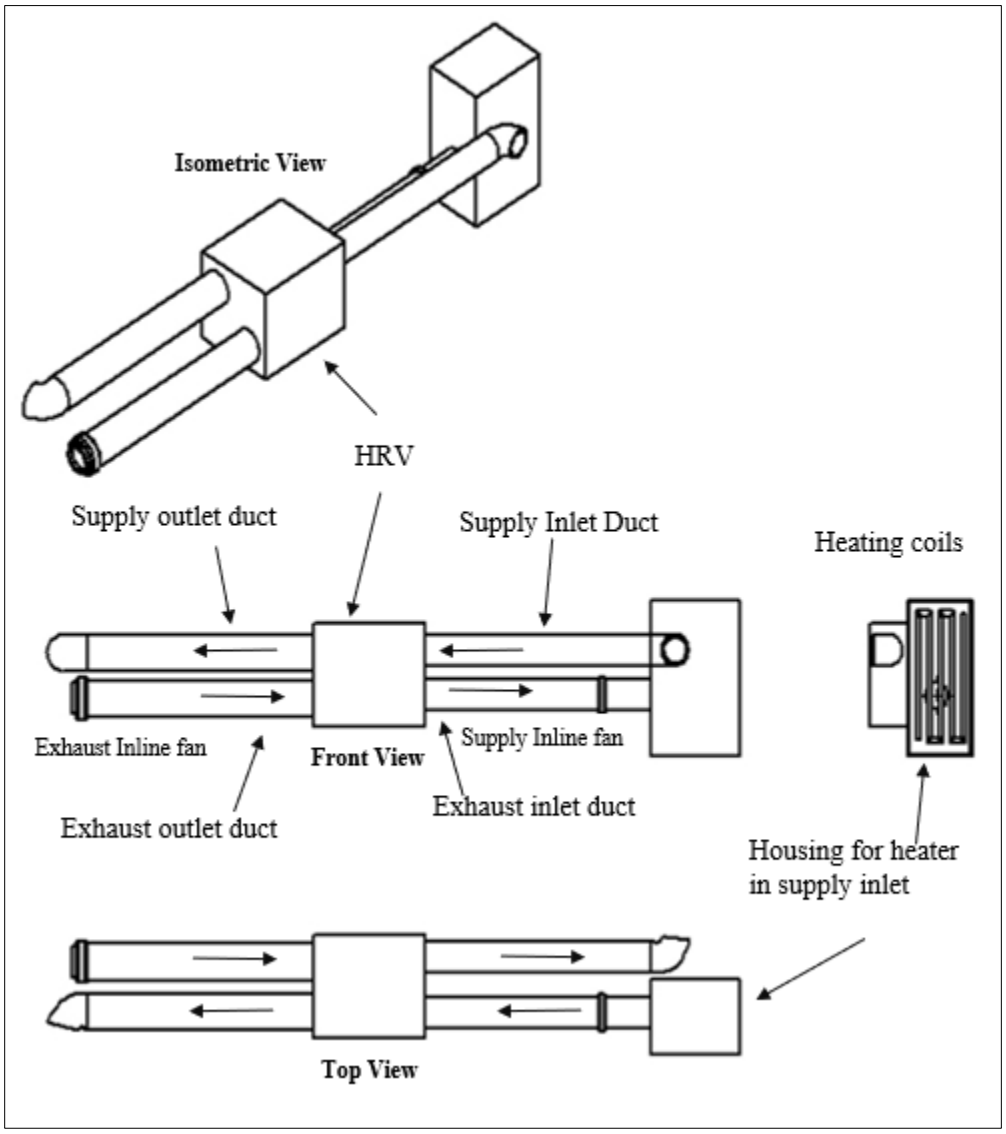

Figure 1 3D drawing of the testing facility

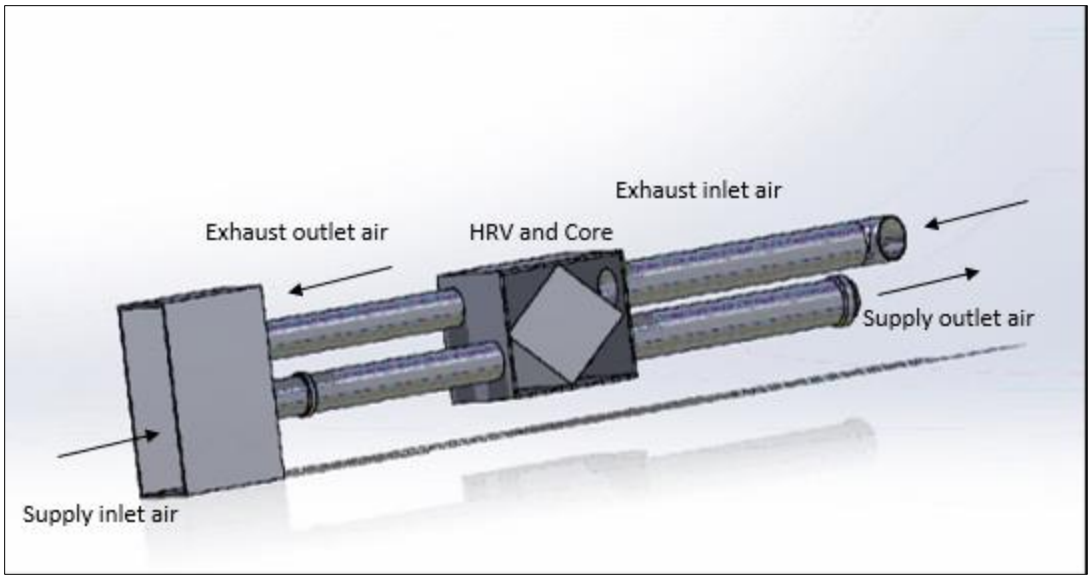

Figure 2 3D model of the Unit visualized in SolidWorks

facility construction began. An essential initial step in the design process before fabricating the REEL testing facility was the development of a 3D model of the HRV testing setup and unit by using SolidWorks visualization, as shown in figure 1 and figure 2.

The ducting system and its attachments that connect the HRV unit to the inlet and outlet can be easily seen in Figures 1 and 2. In order to provide compatibility with most of the HRVs in the market, each circular duct's diameter is 6 inches, and the length is assigned to be 103 inches long. The 103-inch lengths of circular ducts attached to the inlet and outlet ports of the HRV provide a path to ventilate the outdoor and conditioned air while making room for installing temperature, humidity, and flow rate sensors to simulate indoor and outdoor conditions. This length is also important for achieving a fully developed flow upstream of the unit and the instruments. Furthermore, the ducts are fabricated using sheet metal with elbows attached to the extreme ends to avoid mixing conditioned air and treated air by aligning the elbows 180° from each other.

A rectangular duct, measuring $23.5\ inches \times 12\ inches$, is attached to the inlet of the supply duct, which also houses the heating coil while allowing enough space for a smooth airflow without

interruptions. The heating coil, which is shown in Figure 3, is placed 13.7 inches from the rectangular duct's inlet. Axial inline fans are attached to the terminals of the supply and exhaust inlet ducts to achieve varying airflow rates and receive power from a variable transformer or Variac. The inline supply fan draws in air heated by the heating coils.

Figure 3 Heating coil in the rectangular duct

An important feature of the REEL testing facility design is to provide flexibility for mounting thermal recovery units following the manufacturer's instructions. A steel structure that includes three degrees of freedom was designed and installed in order to allow the HRV to be wall, ceiling, or floor mounted. As an example, Figure 4 shows the unit is hung from the ceiling with chains above the ground where the ducts and HRV ports can be aligned to the unit without moving the ducts and ports.

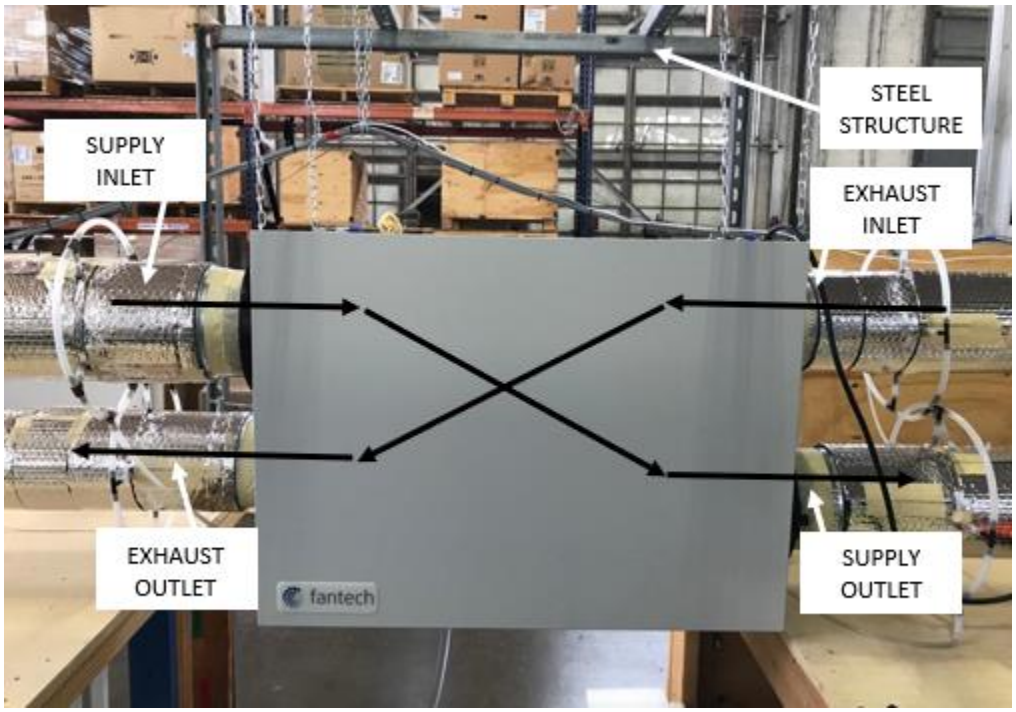

Figure 4 Steel structure with ceiling mount procedure as instructed by the manufacturer

2.2. MEASURING DEVICES AND SPECIFICATIONS

Each duct in the facility contains five sensors: a velocity meter, temperature sensors, CO_2 sensors, Relative Humidity (RH) sensors, and static pressure taps with RH and CO_2 sensors being a

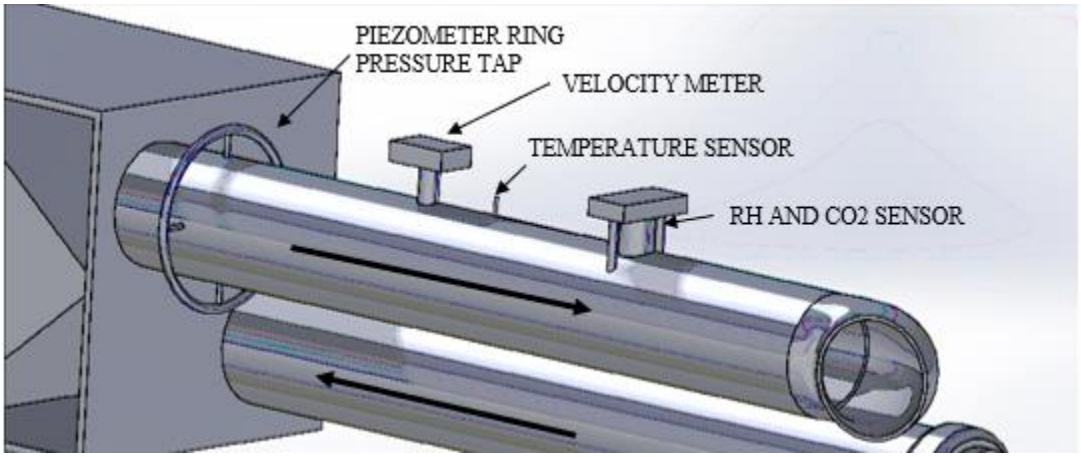

Figure 5 3D model of sensors installed in the testing facility

combined unit. These sensors are used to obtain data to determine the psychrometric states, CO_2 concentration, volumetric flow rates of air in each duct along with the thermal performance, SHRE,

and the Effectiveness of the HRV unit. The 3D model, in Figure 5, shows the locations of all five sensors that are incorporated in the new facility for HRV testing.

2.2.1. AIR VELOCITY SENSOR

The EE650 air velocity transmitter, which is often used for HVAC applications, measures airflow velocity in all four ducts connected to the HRV unit, and they are positioned 64 inches from the exposed ends of the duct. The volumetric flow rate is then determined by knowing the cross-sectional duct area. A picture of the sensor is shown in figure 6, and the specifications of the airflow sensor, along with all the other sensors, are tabulated in Table 1.

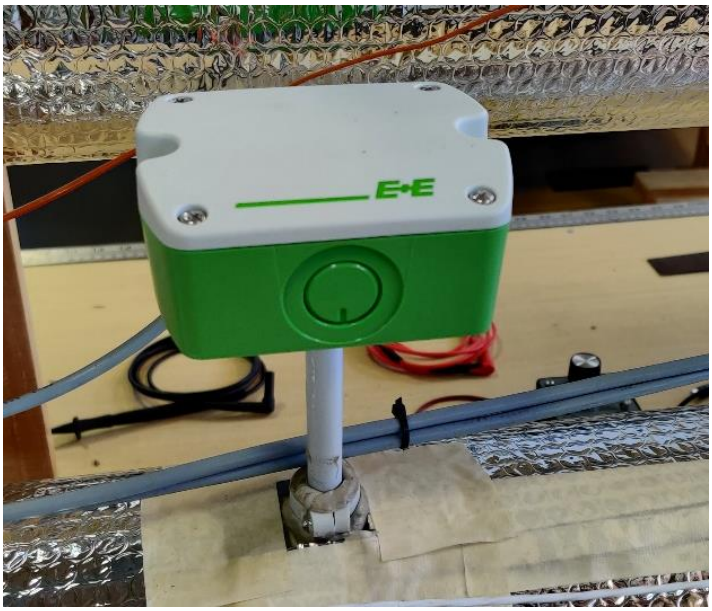

Figure 6 Air velocity meter

2.2.2. RELATIVE HUMIDITY AND CO_2 SENSOR

A Dwyer CDTR-2D4D4 sensor, shown in Figure 7, is used to measure CO_2 and relative humidity in a combined unit, in each of the four duct segments, in the testing facility, with the sensor positioned 30 inches from the exposed end of each duct. Of particular importance, the psychrometric properties of air are determined with the help of the RH sensor while the mixing

parameter occurring at the exhaust outlet and supply inlet is determined by using CO_2 measurements. The specifications of the measuring device are tabulated in Table 1.

Figure 7 CO2 and RH sensor

2.2.3. THERMOCOUPLE

Omega T-type thermocouples, shown in Figure 8, are used to measure the temperature of the air moving through each of the four ducts with temperature representing values entering and exiting the HRV unit in each case. The thermocouples are placed 40 inches from the exposed end of each duct, and their specification are shown in Table 1.

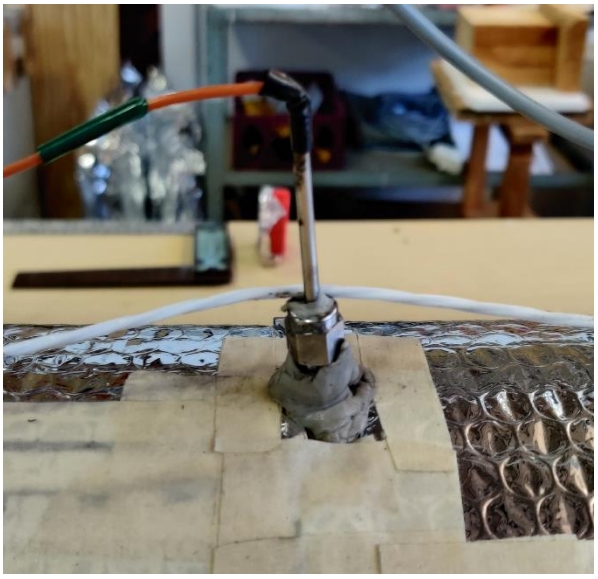

Figure 8 Thermocouple

2.2.4. PRESSURE TRANSDUCER

The Setra 2641003WD11T1F sensors, shown in Figure 9, are used to measure the static pressure difference across the HRV unit with the pressure drop occurring in each of the two flow streams being an important performance parameter. The pressure taps connected to the transducer are placed 6 inches from the ports of the HRV and specification details of the measuring device are shown in Table 1.

Figure 9 Pressure Transducer

It is important to note that the above pressure transducer is connected to the piezometric ring pressure taps installed around the duct for the purpose of determining the air's static pressure inside the duct. The Piezometer ring pressure taps are built in-house, following instructions from the AMCA 210, Laboratory Methods of Testing Fans for Ratings with important dimensions of the pressure taps depending on the duct's dimensions, which is installed as shown in Figure 10.

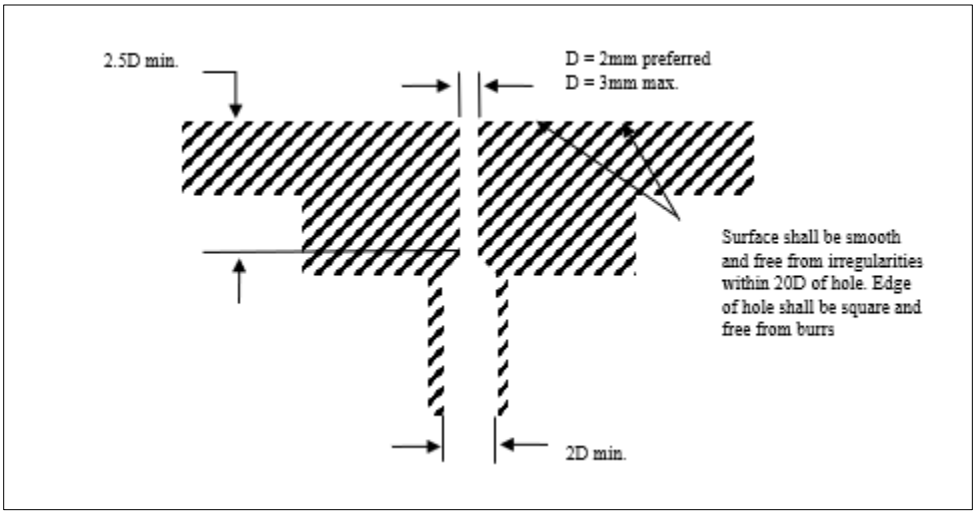

Figure 10 Piezometer ring pressure tap schematic

All the sensors are connected to the Data Acquisition System, which provides raw data to the user interface software, LabVIEW, to be interpreted. Consolidated list of all sensors is tabulated in Table 1.

Table 1 List of all sensors used in the REEL testing facility

Sensors	Range	Accuracy	Output	Temperature Range
Air Velocity meter	0-10 m/s	0.2 – 10 m/s ± (0.2 m/s ± 3% of m.v.)	Analogue, 0 – 10 V, 4 – 20 mA	-

Table 1 Continued

Sensors	Range	Accuracy	Output	Temperature Range
CO_2 and RH Sensor	0 – 5000 ppm	40 ppm 3% of reading	0 – 5 VDC/ 0 – 10 VDC / 4 – 20 mA	32°F to 122°F
Thermocouple	-250°C to 350°C	$\pm 1°C$ or $\pm 0.75\%$	-6.258 mV to 20.872mV	-250°C to 350°C
Pressure Transducer	0 – 3 inches of water	0.25 %	4 – 20 mA, 0 – 800 Ohms	-18°C to 79°C.

3. TEST PREPARATION

3.1. MASS BALANCING OF SUPPLY AND EXHAUST

Airflow mass balancing of the two sides of the ventilation unit, namely the supply and exhaust, is essential in achieving high heat transfer between two opposite flowing streams and thus sustaining healthy inhabitable indoor spaces. The CSA C439 standard specifies that HRV testing conditions are valid only when the supply and exhaust flow rates in each of the inlet and outlet ports are within a 3% tolerance of the average taken from all the flow rates through the HRV/ERV.

The average is calculated over 10 minutes of data as specified by the C439 standard.

$$Average\ CFM\ = \frac{Supply\ inlet + Supply\ outlet + Exhaust\ inlet + Exhaust\ outlet}{4} CFM$$

Valid conditions are met if

$$(|Supply\ inlet\ CFM - Average\ CFM|) \leq 3\%\ of\ Average\ CFM$$

$$(|Supply\ outlet\ CFM - Average\ CFM|)\ \leq 3\%\ of\ Average\ CFM$$

$$(|Exhaust\ inlet\ CFM - Average\ CFM|)\ \leq 3\%\ of\ Average\ CFM$$

$$(|Exhaust\ outlet\ CFM - Average\ CFM|) \leq 3\%\ of\ Average\ CFM$$

A difference between individual flow rates and the average of four flow rates, greater than 3%, is considered unacceptable. To ensure balancing the HRV ventilation rates, auxiliary systems consisting of dampers and axial inline fans were installed in the testing facility as shown in Figure 11. Specifically, balanced ventilation across the HRV was achieved at multiple speeds by performing and analyzing numerous iterations in damper and axial fan control modifications. The introduction of axial inline fans in the supply inlet duct and exhaust inlet duct also helped achieve

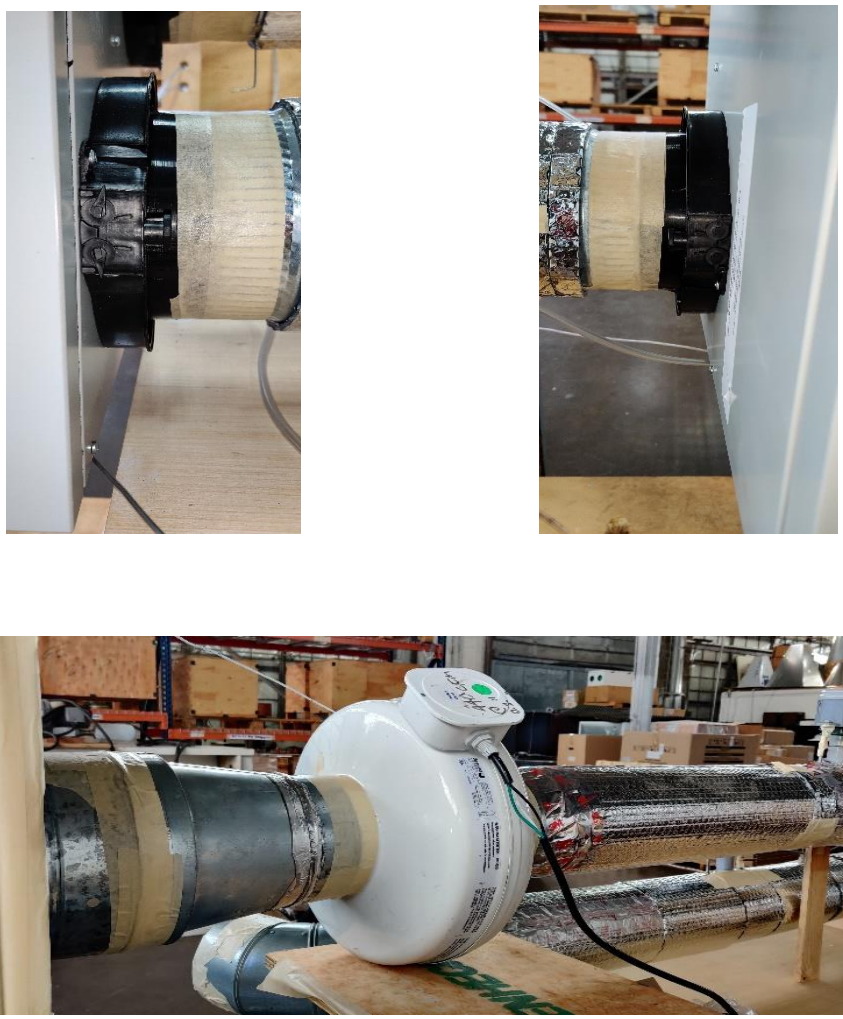

Figure 11 System of Dampers and Axial fans to regulate airflow in ducts

high volumetric flow rates inside the supply and exhaust ducts. Additionally, HRV's in-built collar dampers and external dampers were adjusted to attain various HRV/ERV flow rates.

A sample of volumetric flow rate data collected over a 30-second period is shown in Table 2, with the percentage error in the individual flow rates with respect to the average flow rate in four ducts. Initially, the average percentage of errors in the volumetric flow rates at a rated 102 CFM speed were 6.61 %, 5.30%, 1.74%, and 1.07% in the four ducts, making this particular test invalid as the supply/exhaust inlet percentage of errors are a little beyond the 3% tolerance limit.

Table 2 Example of unbalanced airflow at 106 CFM flow rate

	CFM					% difference in CFM			
Time Elapsed (s)	Supply Inlet	Exhaust Inlet	Supply Outlet	Exhaust Outlet	Average	Supply Inlet	Exhaust Inlet	Supply Outlet	Exhaust Outlet
2	112	101	104	108	106	5.30%	4.78%	2.28%	1.77%
4	114	101	105	107	107	7.25%	4.50%	1.54%	1.20%
6	114	102	105	107	107	7.52%	3.86%	1.45%	1.14%
8	114	101	104	107	107	7.14%	4.51%	1.67%	0.90%
10	114	101	104	107	107	7.18%	5.11%	1.83%	1.03%
12	114	101	104	107	107	6.91%	4.94%	1.81%	1.20%
14	114	101	104	108	107	6.90%	5.13%	1.69%	1.24%
16	114	100	104	107	106	6.94%	5.50%	1.79%	1.16%
18	113	100	104	107	106	6.83%	5.58%	1.81%	1.19%
20	113	100	104	107	106	6.69%	5.77%	1.80%	1.09%
22	113	100	104	107	106	6.70%	5.90%	1.62%	0.94%
24	113	100	104	107	106	6.26%	5.97%	1.85%	0.88%
26	113	100	104	107	106	6.02%	6.19%	1.84%	0.76%
28	112	100	104	107	106	5.92%	6.07%	1.74%	0.77%
30	112	100	105	107	106	5.62%	5.81%	1.42%	0.82%

After balancing the airflow across the HRV, the percentage error dropped to an average of 0.57%, 1.52%, 1.90%, and 2.19% (Table 3). This specific mass balancing was the result of damper alignment and the addition of axial inline fans. The Table 3 results are particularly important to

the research performed herein, because it shows that the balancing procedure developed at REEL by using a combination of dampers and inline axial fans can be successfully implemented. The reason for using a 30-second interval is that it is not likely that an unbalanced flow be transformed to a balanced flow without the help of damper or axial inline fans whose results are presented in Table 3.

Table 3 Example of balanced airflow at 102 CFM flow rate

	CFM					% difference in CFM			
Time Elapsed (s)	Supply Inlet	Exhaust Inlet	Supply Outlet	Exhaust Outlet	Average	Supply Inlet	Exhaust Inlet	Supply Outlet	Exhaust Outlet
2	102	104	99	104	102	0.17%	1.29%	2.74%	2.74%
4	102	103	99	105	102	0.06%	1.29%	2.47%	2.58%
6	102	103	100	105	102	0.44%	1.12%	2.05%	2.43%
8	103	103	100	105	103	0.31%	1.15%	2.32%	2.56%
10	102	103	100	105	102	0.25%	1.25%	2.21%	2.26%
12	102	103	100	104	102	0.13%	1.30%	2.02%	2.12%
14	102	103	100	104	102	0.30%	1.29%	1.98%	2.03%
16	102	103	100	104	102	0.31%	1.27%	2.01%	2.12%
18	102	103	100	104	102	0.40%	1.28%	2.08%	2.01%
20	102	103	100	104	102	0.48%	1.33%	2.04%	2.12%
22	103	103	100	104	103	0.41%	1.35%	1.90%	2.07%
24	102	103	100	104	103	0.56%	1.38%	2.00%	2.28%
26	103	103	100	104	103	0.45%	1.49%	2.07%	2.32%
28	103	104	100	104	103	0.57%	1.52%	1.90%	2.19%
30	103	104	100	104	103	0.62%	1.50%	1.87%	2.27%

The previous two tables showed how balancing could be achieved for one specific flow rate at around 100 CFM, but the same procedure was used for airflow rates from 85 CFM to 235 CFM with the resulting percentage of error for the speeds tabulated in Table 4. As seen in Table 4, there were only six instances where the individual volumetric flow rate exceeded the 3% tolerance, with two pairs of the six readings belonging to the same CFM. There are only four out of ten tests in Table 4 that are to be considered invalid. Even so, with additional balancing efforts using dampers and axial inline fans one would expect valid balancing to be achieved.

Table 4 Percentage error in airflow rates

Average CFM in all four ducts	Supply Inlet % difference	Exhaust Inlet % difference	Supply Outlet % difference	Exhaust Outlet % difference
86 CFM	2.134%	0.813%	0.313%	0.823%
103 CFM	0.019%	1.918%	2.078%	2.373%
121 CFM	4.907%	2.030%	0.841%	3.167%
137 CFM	1.599%	1.837%	0.335%	0.747%
154 CFM	2.925%	0.355%	0.485%	3.760%
176 CFM	1.307%	1.558%	1.658%	3.307%
194 CFM	0.498%	0.505%	3.099%	3.244%
210 CFM	0.599%	1.244%	1.383%	2.034%
219 CFM	0.191%	0.291%	1.322%	1.615%
233 CFM	2.667%	2.261%	2.755%	2.616%

3.2. AMBIENT CONDITIONS

As per C439 standards, the ambient conditions for each and all testing should be maintained at 22 $\pm$ 3˚ C dry bulb temperature and 40 $\pm$ 5 % RH while determining the volumetric flow rates, SHRE, and effectiveness of the HRV.

3.3. SYSTEM CHECKS AND LAB TESTING PROCEDURE

A major goal of this thesis is to develop a testing facility to obtain performance results for HRVs faster than the conventional "cooling mode" approach. An important criterion is that the equipment to be tested shall be operated after thermal and airflow equilibrium conditions are achieved. With data being recorded at intervals of 10 minutes after an hour of warmup. During the "cooling mode" conditions, the tests shall be performed with an exhaust inlet air temperature of 24 ˚C dry-bulb and 50 % RH. These conditions were already met in the lab with the help of an industrial air conditioner. The supply inlet (outdoor) air temperature shall be 35 ˚C dry-bulb and 50 % RH. This temperature was achieved by using a heating coil with a PID controller placed in the rectangular duct before the circular supply inlet duct.

The time-averaged temperature of supply inlet air should be within $\pm 0.5°C$. Specifically, the maximum and minimum of the average temperatures allowed after 10 minutes of collecting data in the "cooling mode" testing condition should be 35.5°C and 34.5°C, respectively. Instantaneous values of supply and exhaust temperatures should be within $0.4°C$ of 35°C. The unit shall be tested at 60 Hz and 120 V AC $\pm$ 1% (or at another supply voltage specified by the manufacturer).

The C439 standard requires that the absolute static pressures in the inlet and outlet ports be the same in both supply and exhaust ducts. Data shall be collected at intervals of 25 pascals or 0.1 inches of water for the volumetric flow of up to 100 L/s or 211 CFM and 50 pascals or 0.2 inches

of water for the volumetric flow greater than 100 L/s or 211 CFM as shown in Table 5 with stations defined in Figure 12.

Table 5 Static pressures corresponding to different flow rates at each station

	STATIC PRESSURE, PASCAL	
STATION	Rated flow up to 100 L/s	Rated flow 100 L/s and over
1	-25	-50
2	+25	+50
3	-25	-50
4	+25	+50

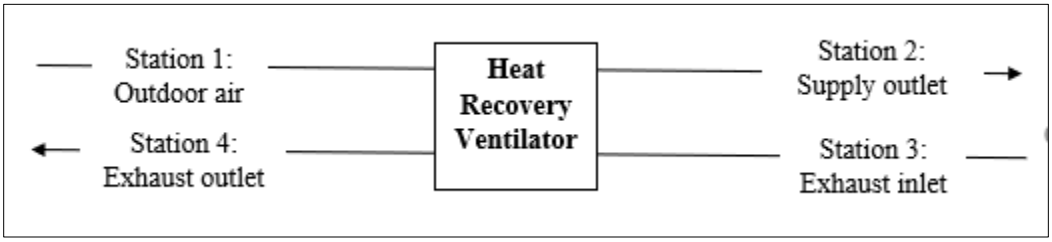

Figure 12 HRV airflow direction

The absolute values of static pressures at “Station 1” and “Station 2” should approximately be the same with uncertainties yet to be determined. Similarly, the absolute values of static pressure at “Station 3” and “Station 4” should approximately be the same. These specific static pressure values can be obtained by modifying the damper arrangement and by increasing or decreasing the inline axial fan’s potential supply. The test shall not be performed if the absolute values of static pressures

are less than those specified in Table 5 or they can be performed by using a revised maximum rated airflow provided by the manufacturer.

Two critical criteria must be met to validate the pressure readings from the pressure transducer. Firstly, the pressure transducer must-read 0 inches of water when disconnected from the piezometer ring pressure taps and exposed to the environment. Secondly, the pressure readings from the transducer must match the pressure readings from a pressure calibrator. If the first case is violated, the transducer may be adjusted to read 0 inches of water when exposed to the environment. If the second case is violated, then there might be an issue with the scaling factor coefficient that converts the electrical signals to readable data. The scaling factor coefficient can be determined by data calibration using the Calibration wizard tool in LabVIEW (as shown in Figure 13), a pressure calibrator, and a pressure pump.

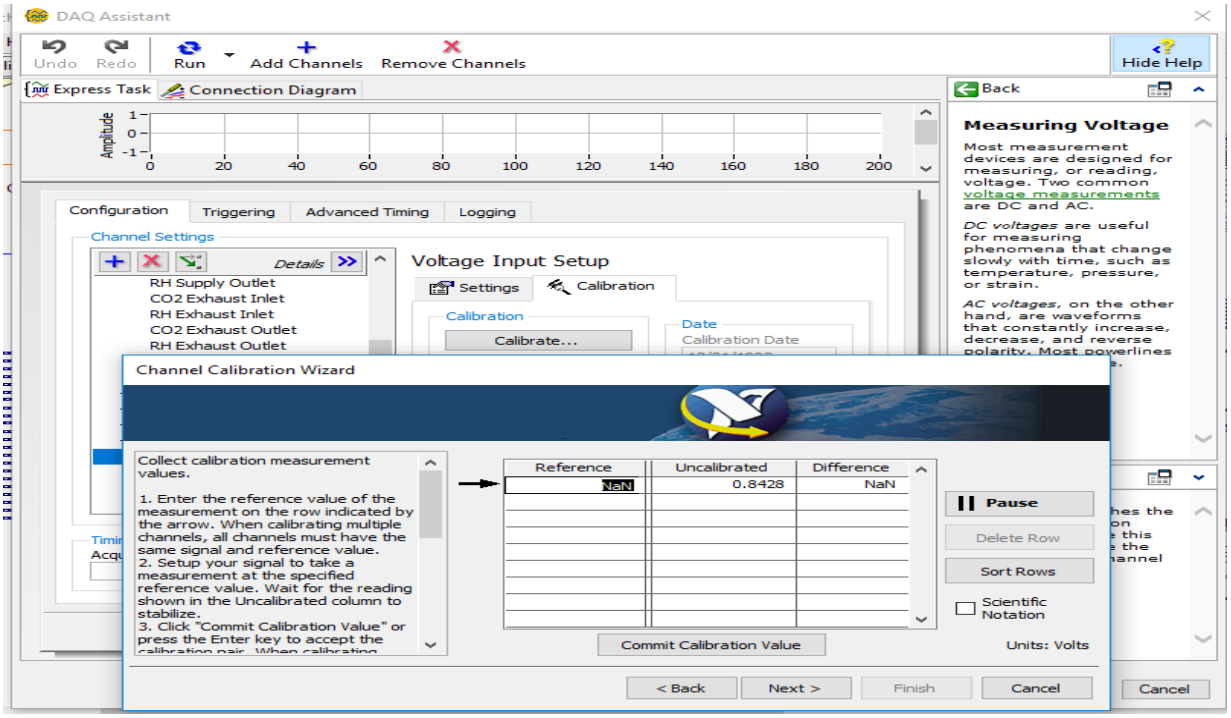

Figure 13 Calibration wizard user interface in LabVIEW

The pump is connected to the pressure transducer and a pressure calibrator, and then the electrical signal from the transducer is compared with the static pressure reading from the pressure calibrator.

The electrical signal corresponds to a unique static pressure value and produces a linear curve when plotted. The regression equation that follows the trend of the curve gives the scaling factor. The scaling factor may be registered into the LabVIEW program to show the correct static pressure values. Once it is certain that the pressure values are credible, data collection may begin. Ten minutes of data shall be recorded and read simultaneously into an excel spreadsheet. The path where the data should be stored is also mentioned in the user interface.

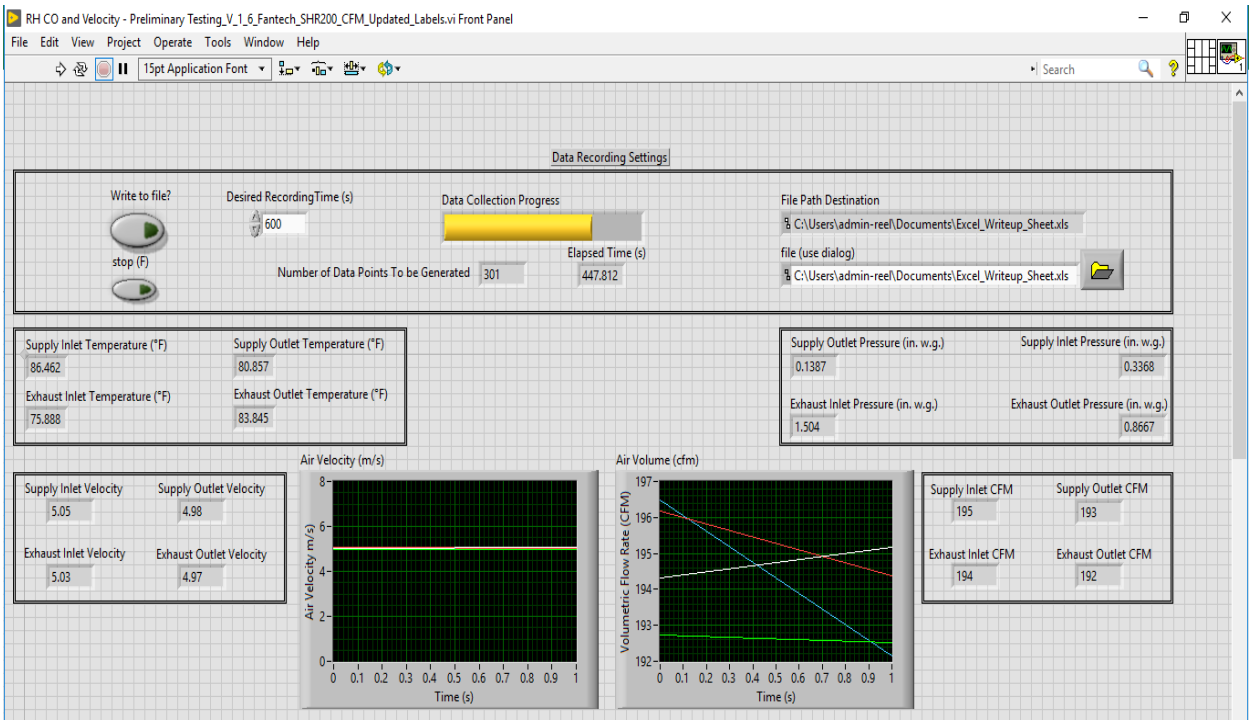

Figure 14 REEL HRV Testing software user interface

4. OBSERVATION AND RESULTS

4.1. ENERGY PERFORMANCE OF HRV

The energy performance of an HRV is measured by the values of the Sensible Recovery Heat Efficiency (SHRE) and the effectiveness at any given flowrate. Effectiveness is defined as the ratio of actual heat transfer to the maximum thermodynamically limited heat transfer possible. In contrast, SHRE is defined as the apparent effectiveness when external gains, internal gains, and losses are considered in the equation. These gains can be due to fan energy, imbalance in the airflow, air leakage, and frost control. Therefore, as a major contribution of this study, the SHRE and effectiveness of the Fantech SHR 200 HRV were determined at the rated flow of 195 CFM.

The first step in determining the Energy Performance of the HRV is measuring and recording the dry-bulb temperature of air, mass flow rates, and the power drawn by fans and the HRV. Data is recorded through the data acquisition system and stored in an excel spreadsheet on the computer. Additionally, the power drawn by the fans and the HRV was found manually by using a current clamp meter. The raw data is then processed to calculate SHRE and Effectiveness of the HRV. A portion of a 10-minute data set, including the volumetric flow rates and air temperatures in each of the four ducts, is presented in Table 6. It can be seen in Table 6 that over a 10 minute period, the flow rates and temperatures change less than $\pm 1\ CFM\ and\ \pm 0.1\ K$, respectively.

Table 6 Sample data collected for the HRV, at rated volumetric flow and temperature

Volumetric flow rates (CFM)				Air Temperature (°F)			
Supply Inlet	Exhaust Inlet	Supply Outlet	Exhaust Outlet	Supply Inlet	Exhaust Inlet	Supply Outlet	Exhaust Outlet
194	193	187	200	89.7	75.7	84.3	95.8
194	193	187	199	89.7	75.7	84.3	95.8
194	193	187	199	89.7	75.7	84.3	95.8
194	193	187	199	89.7	75.7	84.3	95.8
194	193	187	199	89.7	75.7	84.3	95.8
194	193	187	199	89.7	75.7	84.3	95.8
194	193	187	199	89.7	75.6	84.3	95.7
194	193	187	199	89.6	75.6	84.3	95.6
194	193	188	200	89.6	75.6	84.3	95.6
194	192	187	200	89.6	75.6	84.3	95.7
194	192	188	199	89.6	75.6	84.3	95.7
194	192	188	199	89.6	75.6	84.3	95.8
193	192	189	199	89.6	75.6	84.3	95.9
194	192	189	199	89.6	75.6	84.2	95.9
194	192	189	199	89.6	75.6	84.3	95.9
194	192	189	199	89.5	75.5	84.2	95.8

The mass flow rate in the supply outlet, M_2, is calculated by multiplying the air's density at the instantaneous temperature by the corresponding volumetric flow rate.

$$M_2 = \rho_2(T1) \times V_2$$

Where,

$\rho_2(T1)$ = Density of supply air as a function of temperature, Kg/m^3

V_2 = Volumetric flow rate of air, m^3/s.

The Volumetric flow rate is automatically calculated in the software by multiplying the velocity by the cross-sectional area corresponding to the 6-inch circular duct. It should be noted that dividing the mass flow rate by density can also be used to calculate the volumetric flow rate.

The Effectiveness of the HRV is calculated by using the following formula

$$\boldsymbol{\varepsilon = \frac{M_2 \times (T_1 - T_2)}{M_{min} \times (T_1 - T_3)}}$$

where,

ε = Apparent sensible heat effectiveness

M_2 = Mass flow rate of the supply outlet air, kg dry air per unit of time

T_1 = Dry bulb temperature at the supply inlet, ˚C

T_2 = Dry bulb temperature at the supply outlet, ˚C

T_3 = Dry bulb temperature at the exhaust inlet, ˚C

M_{min} = M_2 or M_4, whichever is less

here

M_4 = mass flow rate of the exhaust air outlet, kg dry air per unit of time

The average temperatures of the supply inlet, supply outlet, and exhaust inlet are used in the equation to determine the effectiveness. **The effectiveness of the HRV at the rated speed of 195 CFM was evaluated and found to be 58%.**

The Sensible Heat Recovery Efficiency (SHRE) of the HRV was calculated by using the following equation,

$$\boldsymbol{E_{SHR} = \frac{(\sum M_{2,i} \times C_P \times (t_{2,i} - t_{1,i}) \times \triangle\theta) - Q_{SF}}{(\sum M_{max,i} \times C_P \times (t_{3,i} - t_{1,i}) \times \triangle\theta) + Q_{EF}}}$$

Here,

E_{SHR} = Sensible heat recovery efficiency

M_2 = Net mass flow rate of the supply air outlet, Kg/s

C_P = Specific heat of air kJ/kg.K

t_2 = Net outdoor airflow temperature at station 2

t_1, t_3 = Dry-bulb temperature at stations 1 and 3, respectively, ˚C

$\triangle\theta$ = Time between flow measurements, s

Q_{SF} = Energy input into supply airstream attributed to fan(s), kJ

M_{max} = M_2 or M_4 , whichever is greater

here

M_4 = net mass flow rate of the exhaust air outlet, Kg/s

Q_{EF} = Energy input into exhaust airstream attributed to fan(s), kJ

The above equation is a modified version of the actual formula defined by the C439 standard,

$$\boldsymbol{E_{SHR}} = \frac{(\sum \boldsymbol{M_{2,i}} \times \boldsymbol{C_P} \times (\boldsymbol{t_{2,i}} - \boldsymbol{t_{1,i}}) \times \triangle\boldsymbol{\theta}) - \boldsymbol{Q_{SF}} - \boldsymbol{Q_{SH}} - \boldsymbol{Q_C} - \boldsymbol{Q_D} - \boldsymbol{Q_L}}{(\sum \boldsymbol{M_{max,i}} \times \boldsymbol{C_P} \times (\boldsymbol{t_{3,i}} - \boldsymbol{t_{1,i}}) \times \triangle\boldsymbol{\theta}) + \boldsymbol{Q_{EF}} + \boldsymbol{Q_{EH}}}$$

$Q_{c,}\ Q_D, and\ Q_L$ denote the casing heat transfer, energy used for defrosting, and heat loss due to case leakage. There was no provision installed for determining the case leakage. Since the HRV was tested between room temperature (24°C) and high temperature (35°C), there was no need for a defrost cycle, and hence energy used for defrosting was considered zero. Ideally, there should not be any air/moisture transfer, air leakage, and casing leakage involved when an HRV runs. These assumptions were made while testing the HRV. Finally, Q_{SH} and Q_{EH} were omitted because there was no additional heat needed to raise the air temperature in the supply or exhaust inlets.

The value of SHRE at the rated 195 CFM flow was found to be 32%, with this SHRE being calculated by computing the ratio between the sum of all the thermal energy transfers recorded within the stipulated time limit of 10 minutes(as described in the C439 standard) and the sum of the maximum thermal exchange between supply and exhaust duct. Since the inline fans played a crucial role in attaining the rated speed, its contribution also influences the energy performance. The energy contributions by each fan to attain different speeds are given in Table 7.

Table 7 Power drawn by axial inline fans

Supply power (Watts)	Exhaust power (Watts)	Total Power (Watts)
110	110	220
111	111	221
112	159	271
112	183	295
180	199	379
201	215	416
220	282	502
253	321	573
258	341	600
250	337	587

In addition to the above effectiveness and SHRE values at 195 CFM, additional values shown in Table 8 were determined for a range from 86 CFM to 227 CFM. The difference between the supply and exhaust flows is typically 1 to 2 CFM, with the anomaly at 124 CFM supply, which is more than 8 CFM as shown in Table 8. The performance data in Table 8 as a function of flow rates was also plotted in Figure 15. It can be seen that both performance parameters increase as the volumetric flow rates in both supply and exhaust duct increases. The SHRE increases from 16%

to 33% and the effectiveness increases from 45% to 60%. Specifically, one can observe a steep rise in the lower flow rates between 80 CFM to 140 CFM and steady rise from 150 CFM to 226 CFM.

Table 8 Energy performance of HRV at different flow rates

CFM supply	CFM exhaust	(Supply CFM– Exhaust CFM)	SHRE	Effectiveness	$\left(\frac{Effectivness}{SHRE}\right)$
86	86	0	16%	45%	2.81
102	104	-2	24%	49%	2.04
124	116	8*	30%	56%	1.86
136	135	1	33%	55%	1.66
149	153	-4	29%	57%	1.96
174	173	1	33%	58%	1.75
195	193	2	32%	58%	1.81
209	208	1	31%	60%	1.93
218	217	1	31%	60%	1.93
226	227	1	33%	60%	1.81

(*) – invalid test because of excessive supply to exhaust flow rate difference.

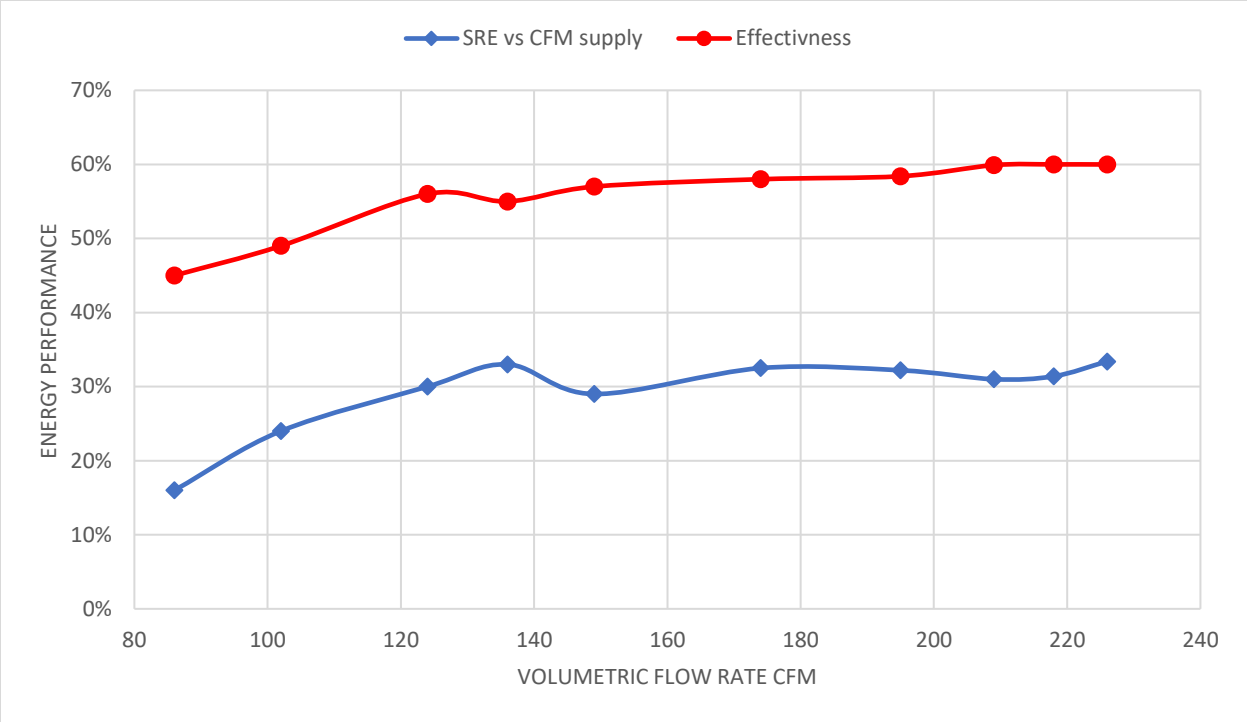

Figure 15 Effectiveness and SHRE Energy performance trend as a function of flow rates

There is an exponential drop in the ratio between Effectiveness and SHRE as seen Figure 16. This drop can be explained by the need for more power by the axial fans as higher CFMs are

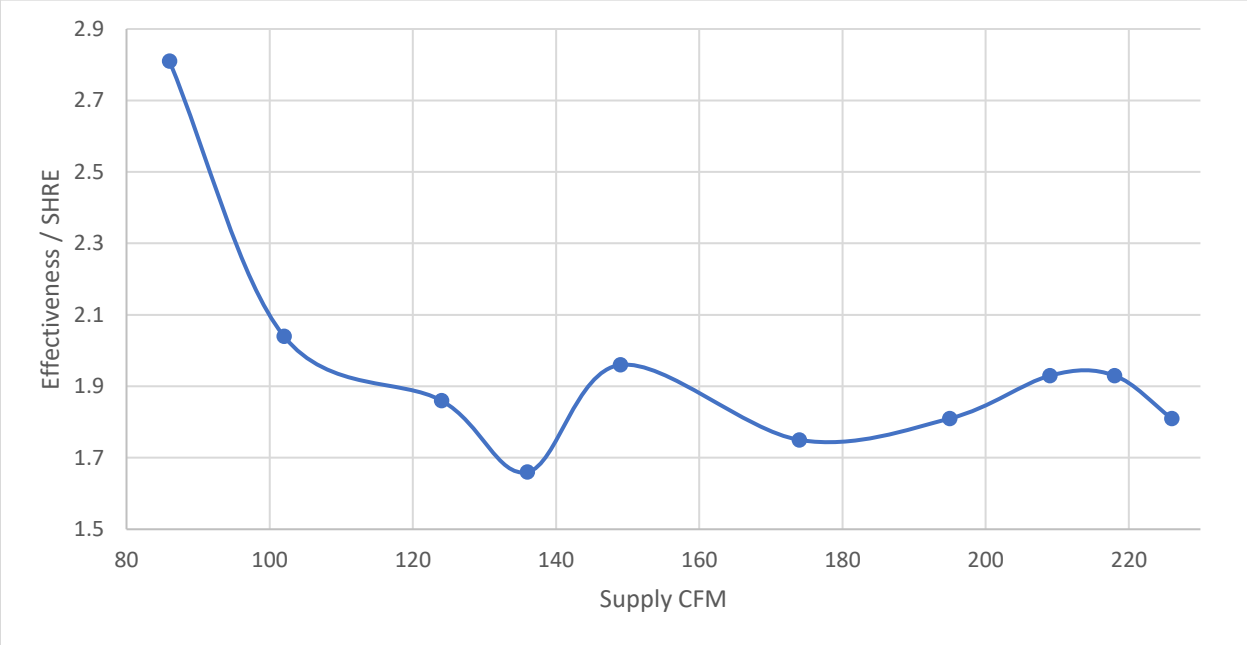

Figure 16 Ratio of effectiveness and SHs and SHRE vs. Supply CFM

approached. An error analysis was conducted on the SHRE and the Effectiveness to determine if

the test results are consistent at various volumetric flow rates. Three tests were conducted for each volumetric flow rate, which totals to 30 tests overall. The standard deviation was found by computing the average of the performance parameters for each of the volumetric flow rates and then they were included in the performance graphs. The standard deviations varied from 0.5 to 3.7% for the SHRE and from 0.2 to 2.3% for the Effectiveness.

Table 9 Average SHRE and corresponding standard deviation at each volumetric flow rate

CFM	SHRE1	SHRE2	SHRE3	Average	Standard deviation
85	16.0%	13.2%	15.0%	14.7%	1.4%
102	24.0%	17.7%	17.4%	19.7%	3.7%
122	30.0%	27.3%	27.2%	28.2%	1.6%
135	33.0%	32.0%	32.2%	32.4%	0.5%
155	29.0%	30.9%	26.7%	28.9%	2.1%
174	33.0%	29.6%	30.6%	31.1%	1.8%
195	32.0%	30.8%	29.8%	30.9%	1.1%
210	31.0%	28.8%	28.5%	29.4%	1.4%
222	31.0%	27.9%	28.3%	29.1%	1.7%
235	33.0%	30.9%	31.2%	31.7%	1.1%

Table 10 Average Effectiveness and corresponding standard deviation at each CFM

CFM	Eff1	Eff2	Eff3	Average	Standard deviation
85	45.0%	43.6%	43.8%	44.1%	0.8%
102	49.0%	45.3%	45.6%	46.6%	2.0%
122	56.0%	52.0%	52.1%	53.4%	2.3%
135	55.0%	55.6%	55.6%	55.4%	0.3%
155	57.0%	57.0%	55.1%	56.3%	1.1%
174	58.0%	57.1%	57.8%	57.6%	0.5%
195	58.0%	58.4%	58.0%	58.1%	0.2%
210	60.0%	58.0%	58.2%	58.7%	1.1%
222	60.0%	58.1%	58.5%	58.9%	1.0%
235	60.0%	57.9%	58.2%	58.7%	1.1%

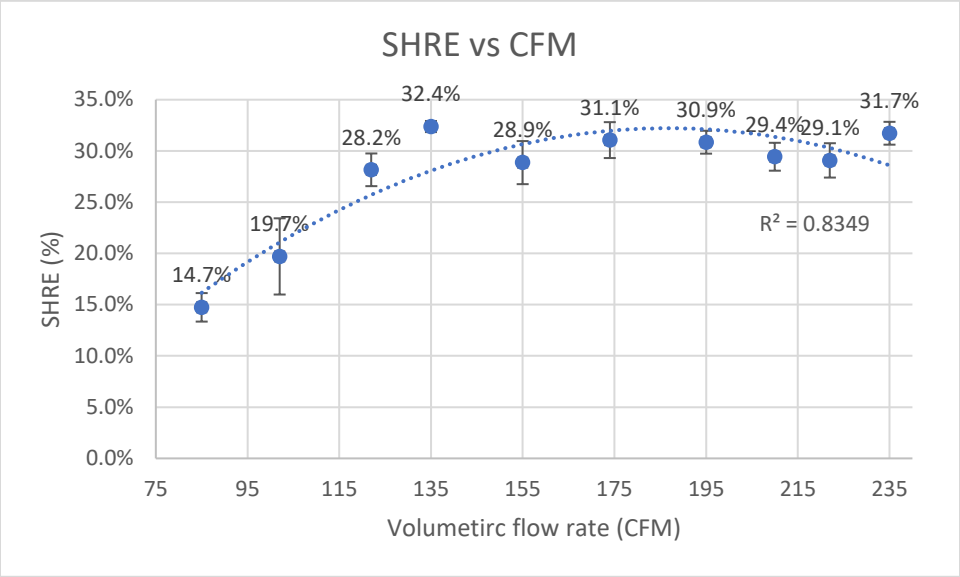

Figure 15 Error plot of SHRE vs Volumetric flow rate

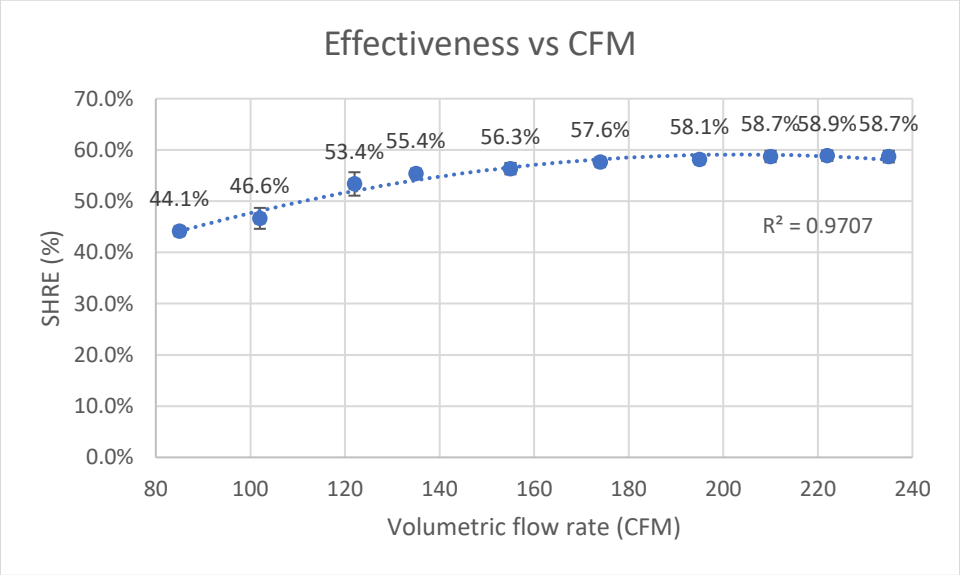

Figure 16 Error plot of Average Effectiveness vs Volumetric flow rate

An airflow performance analysis and thermal performance analysis on the HRV were conducted in addition to the energy performance analysis.

4.2. AIRFLOW ANALYSIS

The objective of this analysis was to determine the relationship between volumetric flow rate and corresponding external static pressures in an HRV system. This analysis evaluated the fan's airflow performance for a set of volumetric flow rates between 85 CFM and 226 CFM, which is a range based on the "HVI documentation report for the Fantech's SHR 200 airflow performance study," and its corresponding static pressure and the external static pressure as measured in the REEL testing lab. According to HVI, external static pressure is defined as follows, "*Total static pressure loss of the exhaust or supply system in the ductwork. In the exhaust system, the total static pressure differential is the static pressure maintained at the exhaust outlet minus the static pressure measured at the exhaust inlet. The supply system's total static pressure differential is the static pressure measured at supply outlet minus the static pressure measured at the static inlet."(hvi tested/certified heat recovery ventilators and energy recovery ventilators (hrv/erv))*

Figure 19 is an example of how external static pressure is calculated. Figure 19 shows the change in static pressure in a series of ducts with a fan. The static pressure in the exposed ends of the ducts is at 0 inches of water. The static pressure drops towards the fan due to friction and bends in the duct and is lowest at the inlet of the fan. The static pressure rises to the highest value at the fan's outlet and drops naturally to 0 inches of water due to bends and friction in the duct.

From Figure 19, the external static pressure is the difference between the static pressure across the HRV. It is to be kept in mind that static pressure taps were installed near the ports only in the actual testing facility. Figure 4.5 is an illustration of how static pressure changes in a system of ducts.

$$External\ Static\ Pressure = Outlet\ static\ pressure - Inlet\ static\ pressure$$

$$0.4 - (-0.23) = 0.63\ inches\ of\ wtaer$$

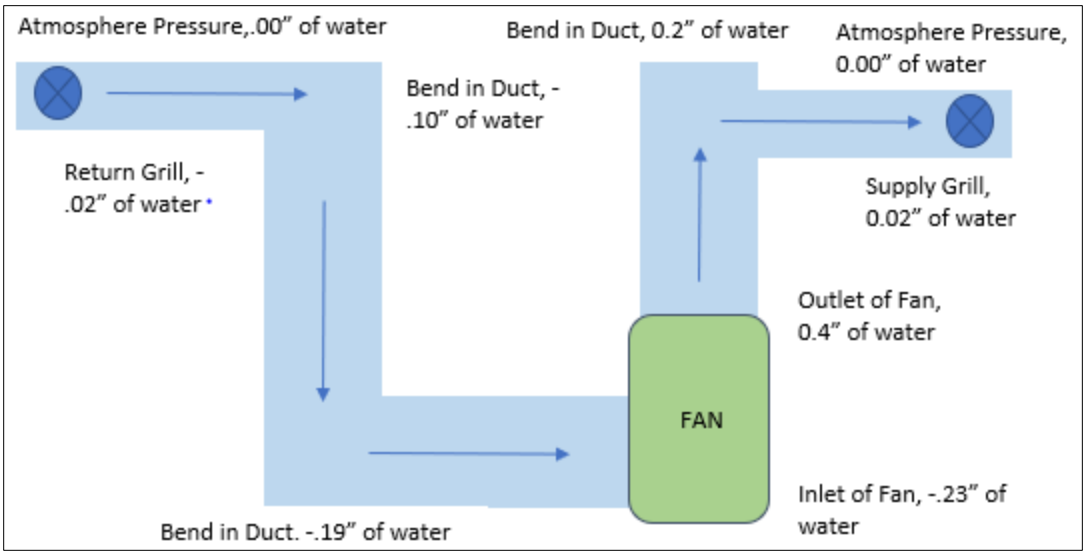

Figure 17 Duct system explaining external static pressure across a fan

Computations, similar to above, were performed for a range of flow rates achieved by using the Fantech SHR 200 HRV and tabulated in Tables 11 and 12 for supply and exhaust static pressures, respectively.

Table 11 Supply static pressure

Supply CFM	Supply inlet static pressure (inches of water)	Supply outlet static pressure (inches of water)	Supply external static pressure (inches of water)
86	-0.07	0.09	0.16
102	-0.06	0.10	0.18
124	-0.04	0.13	0.17
136	-0.04	0.06	0.09

Table 11 Continued

Supply CFM	Supply inlet static pressure (inches of water)	Supply outlet static pressure (inches of water)	Supply external static pressure (inches of water)
149	0.05	0.07	0.02
174	0.14	0.07	-0.07
195	0.28	0.15	-0.13
209	0.34	0.17	-0.18
218	0.34	0.10	-0.25
226	0.31	0.10	-0.21

Table 12 Exhaust static pressures

Exhaust CFM	Exhaust inlet static pressure (inches of water)	Exhaust outlet static pressure (inches of water)	Exhaust external static pressure (inches of water)
86	-0.21	0.53	0.74
104	-0.12	0.48	0.60
116	0.18	0.61	0.42
135	0.42	0.67	0.35
153	0.85	0.84	-0.01
173	1.01	0.75	-0.26
193	1.45	0.88	-0.58
208	1.71	0.95	-0.76
217	1.83	0.98	-0.85
227	1.78	0.76	-1.01

To provide additional insight into static pressure and flow rates, the static pressure in the supply duct was plotted against the supply volumetric flow rate in Figure 21 and, similarly, Figure 20 for the static pressure in the exhaust duct. The supply inlet static pressure and the exhaust inlet static pressure increases when the volumetric flow rate increases. In Figures 20 and 21, it can be seen that the static pressure curves meet at around 150 CFM.

According to the standard C439, the absolute static pressure readings across the HRV should approximately be the same. If both the static pressures are plotted against one another, a symmetric curve should be observed between Static pressure vs. CFM in a graph, which was not the case, as shown in Figure 20 and Figure 21.

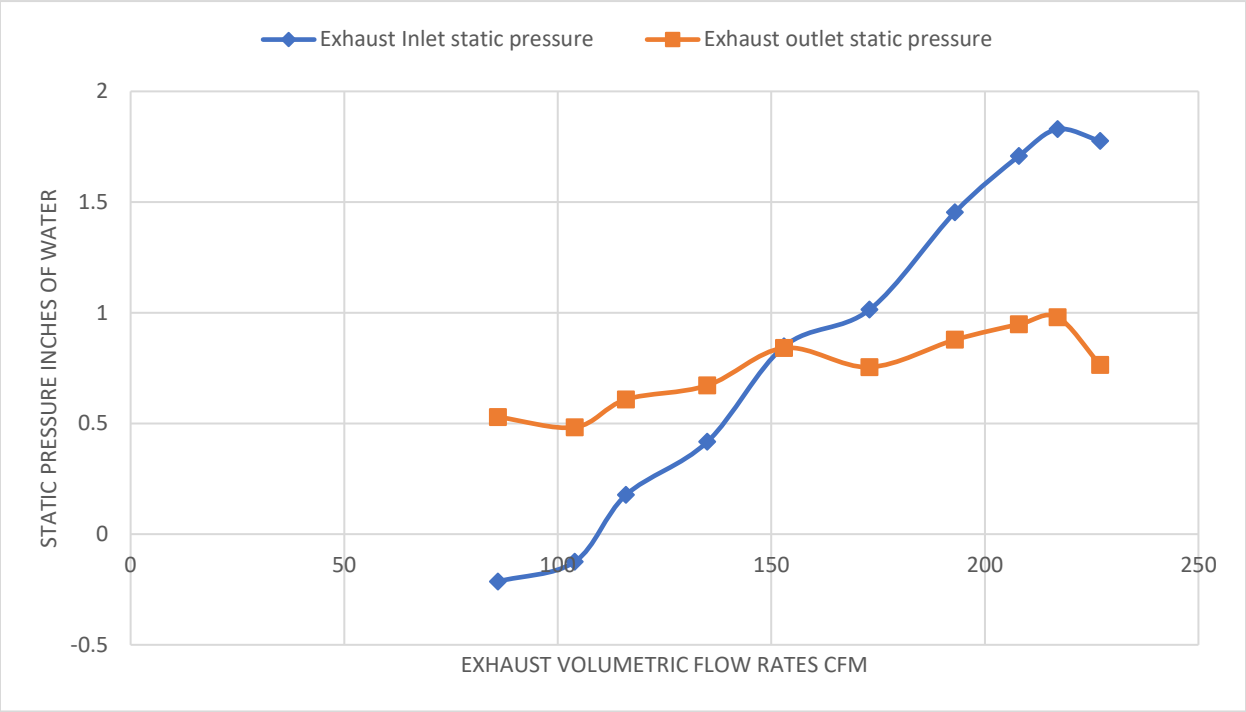

Figure 18 Exhaust static pressure vs. Volumetric flow rate

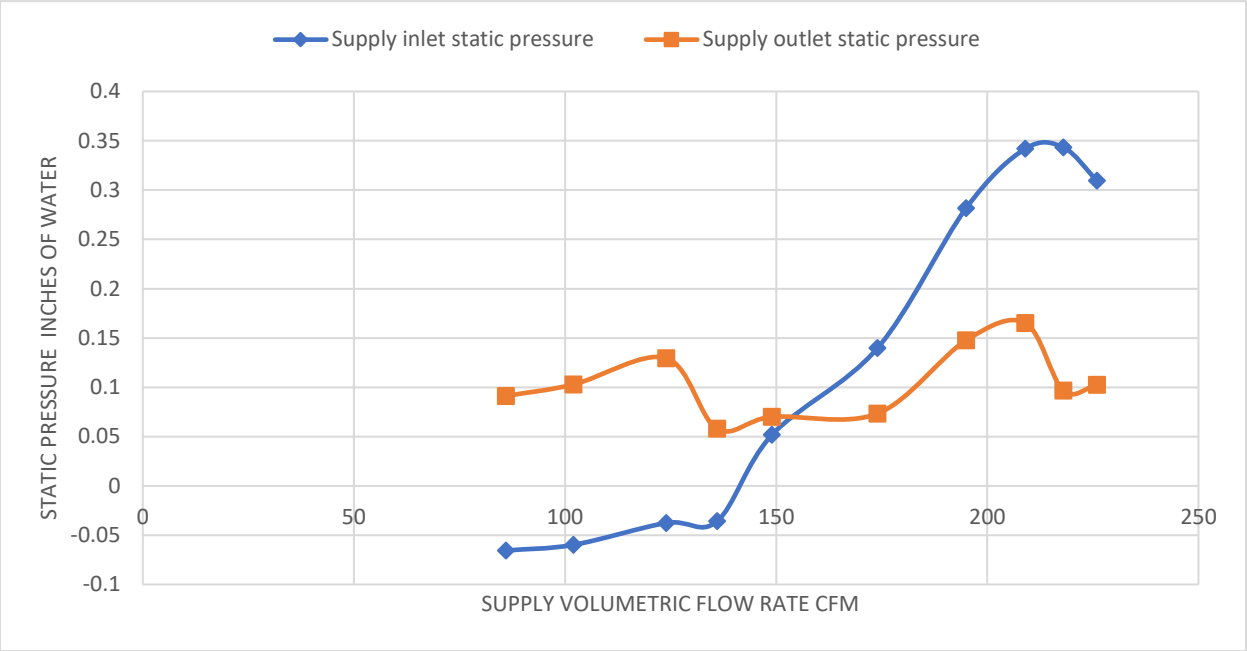

Figure 19 Supply static pressure vs Volumetric flow rate

An essential piece of information to note here is that the scale of pressure values in the supply duct is smaller than the scale of pressure values in the exhaust duct. The highest static pressure recorded in the exhaust inlet duct is 1.83 inches of water compared to 0.34 inches of water observed in the supply inlet duct. Another interesting and insightful plot is the outlet/inlet static pressures (i.e., static pressure difference) versus flow rate for both the supply and exhaust ducts, which are plotted in Figure 22.

It can be observed in Figure 22 that at free flow (flow at 0 inches of water external static pressure), the volumetric flow rate is around 150 CFM in both supply and exhaust ducts. The exhaust external static pressure curve is steeper than the supply external static pressure curve, which is an undesirable condition because it is important to maintain similar external static pressures on both the supply and exhaust ducts. Specifically, if undesirable conditions exist in residential

applications, which could result in unbalanced flow rates, the HRV will not perform effectively in

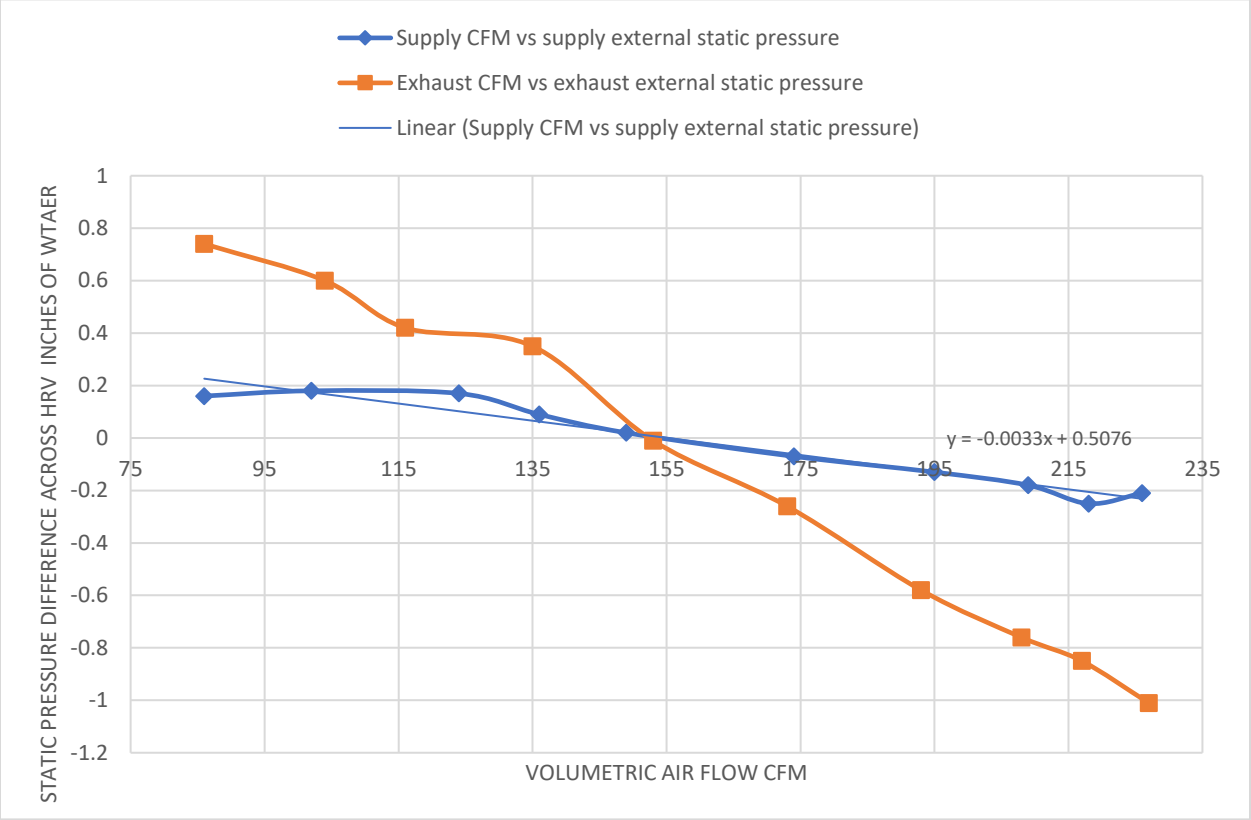

Figure 20 External static pressure vs. Volumetric flow rate

that the thermal zone may pressurize or depressurize, leading to a wastage of energy.

Separate from the HRV testing using the newly built facility, as part of this thesis study was the fan performance tests of the Fantech SHR 200 which was installed and operated in the HRV unit of interest. These fan tests were performed by using an HVI accredited lab, and the fan's airflow performance is plotted in Figure 23. It should be noted that the airflow curves are quite often plotted over a larger CFM flow rate range, starting from 0 CFM; however in this study the fan focus region typically starts at 80 CFM and goes to just over 220 CFM. The performance of supply side fan in the HRV was plotted by using data provided by HVI accredited lab. The exhaust curve is not shown because it traces a similar path as the supply fan curve. The performance of both the fans are similar and almost identical.

The fans installed on both sides of the HRV achieves its rated 195 CFM flow for supply and exhaust external static pressure at 0.4 inches of water as shown in figure 23. With fans installed in

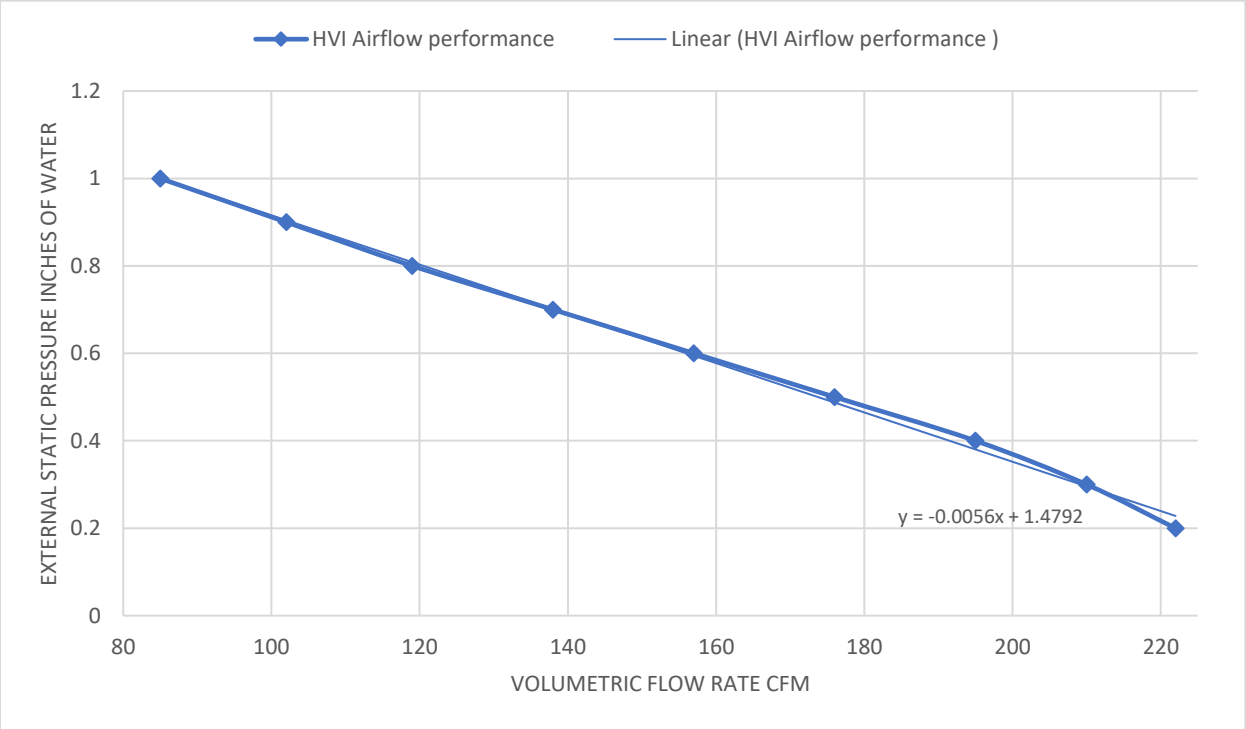

Figure 21 Fan performance curve taken in an HVI accredited lab

both sides of the HRV, the rated speed of the HRV from the REEL testing facility was achieved at a supply external static pressure of -0.13 inches of water and exhaust external static pressure of -0.58 inches of water as shown in Figure 22. Using the curve's regression equation in Figure 23, the volumetric flow rate at free-flow conditions will approximately be 264 CFM. However, after conducting experiments in the REEL testing facility, the regression results show that free flow is achieved at approximately 150 supply CFM.

It would appear that the HRV fan can push more air than what it is capable of at free-flow conditions by at least 100 CFM. This HRV should be able to overcome substantial static pressure interferences in duct systems, as can be seen from Table 13. This lapse in the airflow performance may be attributed to substantial airflow resistance in the duct systems. For example, large pressure drops can occur when the cross-sectional area of duct changes significantly.

Table 13 Comparison of HRV airflow performance

	REEL testing facility	HVI accredited lab	Comment
Free Flow (CFM)	150	264	Volumetric flow rate higher in HVI accredited lab at free flow
External static pressure @ 80 CFM	0.16 inches of water	1 inch of water	Higher external static pressure in REEL testing facility

In the supply side which includes the rectangular duct, the static pressure drop occurs due to friction in the surface of the ducts and due to flow of air from the rectangular duct to the circular duct. The cross-sectional area drops from 294 Sq. Inches to 29 Sq. Inches with almost a 90% abrupt drop in the area is observed as seen in Figure 24.

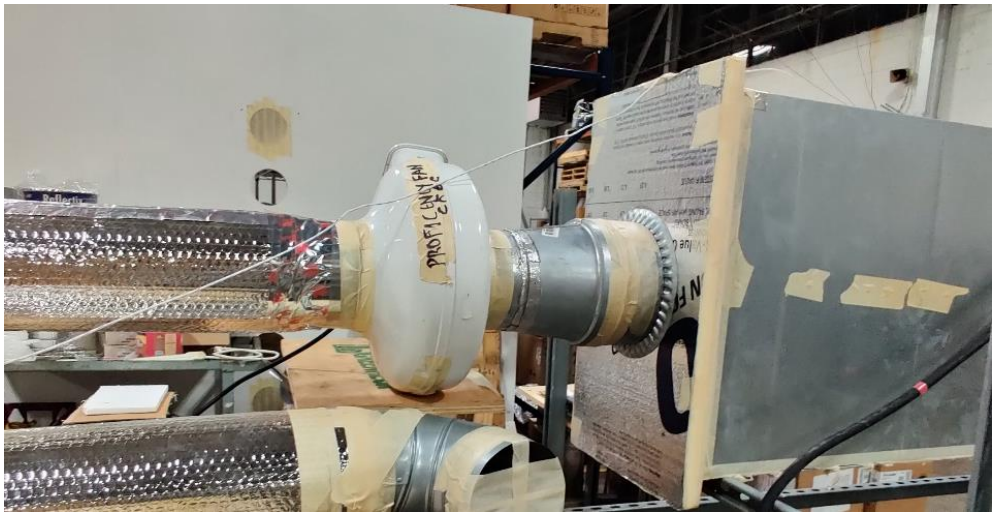

Figure 22 Rectangular duct to circular duct interface

This duct system in the exhaust side is completely circular. The static pressure drop in the exhaust side would be less severe as compared to the static pressure drop in the supply side. Hence, there is a difference in airflow performance between the supply-side and the exhaust-side in the REEL testing facility. The exhaust-side observes 0.74 inches of water external static pressure compared to the lower 0.16 inches of water external static pressure at 86 CFM as seen in Table 11 and Table 12. The comparison is shown in Figure 22. This means there is less resistance to airflow in the exhaust side compared to the supply side. Regardless of the better performance realized in the exhaust side, the overall performance of the HRV as a result of it being tested in the REEL testing facility is lower compared to the performance observed in the HVI accredited lab as seen in Table 13.

4.3. THERMAL ANALYSIS

Standard C439 requires that the outdoor temperature be maintained at 35°C dry-bulb and 50% RH during “cooling mode” testing. The average temperature difference allowed between the supply air inlet and outside air is 0.5°C and the allowed instantaneous temperature difference is 1.5°C. The test is considered invalid if the supply inlet air temperature exceeds the above-mentioned limit. The thermal analysis was done at the HRV’s rated speed of 195 CFM. The supply temperature was difficult to maintain between 34.5°C and 35.5°C and on average, the supply temperature exceeded this tolerance limit by 0.4°C. The PID controller maintained the temperature of the supply air to simulate desirable testing of the outdoor conditions. The supply curve, represented in yellow (Fig.4.9), assumes a sinusoidal behavior. This behavior is due to PID control functions. The indoor temperature was maintained as close to 24°C as possible, with the average temperature being 24.3°C. The average temperature difference between the supply inlet and the supply outlet, T_{supply}, was 6.7°C. The average temperature difference between the exhaust inlet and the exhaust outlet, $T_{exhaust,}$ was 7.9°C at the rated volumetric flow rate of 195 CFM.

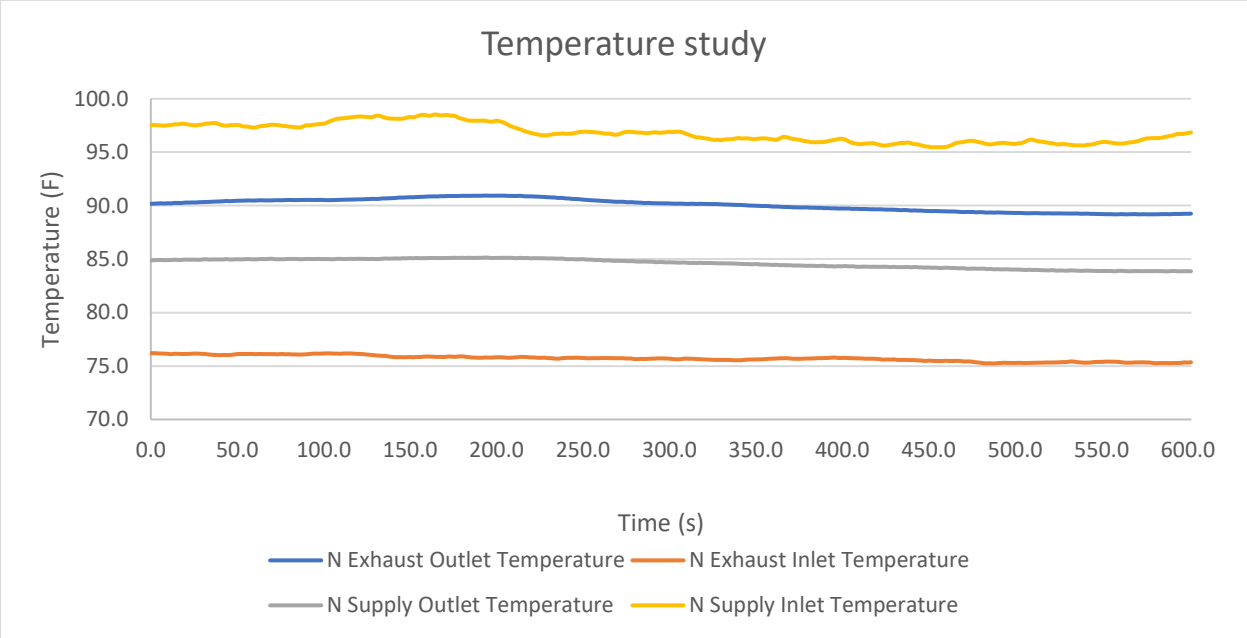

Figure 23 Temperature profile in ducts

Inlet to outlet temperature difference for supply and exhaust sides as function of volume flow rate are tabulated in Table 14 and then plotted in Figure 25. There appears to be a rise in the **Δ**T supply from 4.5°C to 6.7°C as the volumetric flow rises from 85 CFM to 226 CFM. but the opposite trend occurs on the exhaust side where there is a drop in the **Δ**T from 8.2°C to 7.2°C as the volumetric flow rate rises from 85 CFM to 226 CFM. The graph below shows a clear trend in the **Δ**T supply (blue) curve and the subtle negative slope of the **Δ**T exhaust curve (orange).

Table 14 Difference between inlet and outlet temperatures at different volumetric flow rates

CFM supply	CFM exhaust	Supply ΔT (°C)	Exhaust ΔT (°C)
86	86	4.5	8.2
102	104	5.0	8.0
124	116	5.6	8.0
136	135	6.0	7.7
149	153	6.3	7.7
174	173	6.7	8.0
195	193	6.8	8.0
209	208	6.6	7.3
218	217	6.7	7.2
226	227	6.7	7.2

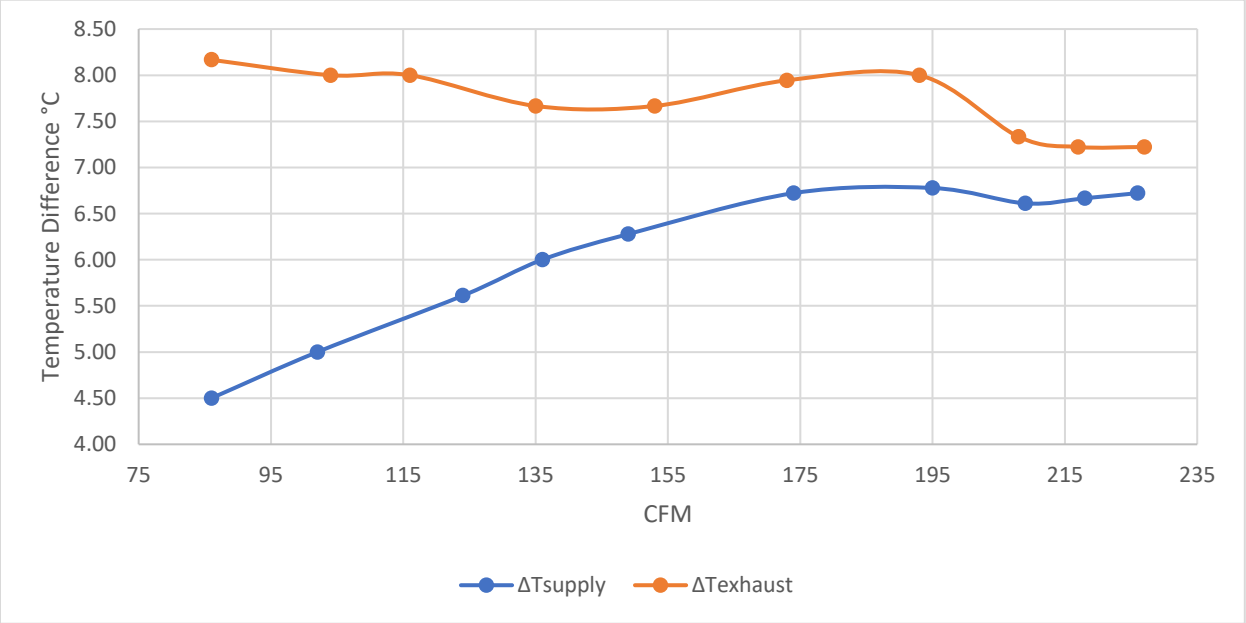

Figure 24 ΔT vs. volumetric flow rate

By intuition, if the flow rate of supply air and exhaust increases, the amount of time there is to exchange heat drops. Hence the ΔT should drop as the volumetric flow rate increases. We can observe two behaviors of trends from the supply side and exhaust side in Figure 26. Knowing that

the supply inlet and exhaust inlet are at constant temperatures of 35°C and 24°C, respectively, the graph indicates that at high flow rates, there is significant drop in the supply outlet temperature. This may be a result of air leakage inside the HRV between the supply stream and exhaust stream. There probably is air movement from supply inlet to exhaust outlet ports, and exhaust inlet to supply outlet ports. This can be seen in the Figure 27.

Figure 25 Core of HRV

5. FUTURE SCOPE

As documented in this thesis, the REEL testing facility can be used to perform “cooling mode” testing, which then leads to energy analysis, thermal analysis, and airflow analysis on HRVs and to obtain full HVI accreditation, the facility must be modified and “heating mode” testing procedures added to expand research capabilities. As an example of modification, a cooling coil must be installed in the supply duct inlet to obtain 0°C and -25°C temperatures.

The current mounting station accommodates units with a port size of 6” in diameter. To accommodate smaller and bigger HRVs in the future, ducts of various cross-sectional sizes must be fabricated and be made available on a standby status.

Apart from HRVs, ERVs are also of interest for HVI certification. Future studies of ERVs, with the goal of obtaining full HVI accreditation for testing and verifying ventilation units, several system modifications are needed, such as steam humidifiers installed to simulate different air humidity levels.

A tracer gas study by using CO_2 should be conducted to monitor the crossflow and leakage of air in the HRV. This type of study would contribute to knowledge of how HRV operations affect Indoor Air Quality (IAQ) of conditioned spaces.

Finally, a detailed, thorough, and comprehensive repeatability test should be conducted to monitor the consistency and accuracy in the data collection and analysis.

6. CONCLUSION

A major focus of this research study has been designing, developing, and constructing a Heat Recovery Ventilator (HRV) testing facility in RELLIS Energy Efficiency Laboratory (REEL), at Texas A&M University, College Station. The REEL testing facility design is based on a significant modification to the CAN/CSA C439, Standard Laboratory Methods of Testing for Rating the Performance of Heat/Energy – Recovery ventilators. The idea behind the modification is to develop a simpler and faster method for testing HRVs in the "cooling mode" (i.e. hot outdoor air temperature and summer conditions), with plans to accommodate "heating mode" (i.e. winter conditions) testing procedures in the future.

Once built and operational, including shakedown tests completed and procedures developed, the research study reported herein then focused on testing and performing extensive energy analysis on the Fantech SHR 200 HRV, which is representative of a typical residential HRV, at its rated 195 CFM speed. These tests produced a large data base and an analysis of it provided an understanding HRV airflow and thermal performance, which has potential for leading to HRV design improvements.

A major contribution of this study is that the Sensible Heat Recovery Efficiency (SHRE) and the Effectiveness of the HRV in the "cooling mode" at its rated 195 CFM volumetric flow rate were investigated by using the data base, and the SHRE and effectiveness were found to be 32% and 58%, respectively. Additionally, these two performance parameters, namely the SHRE and Effectiveness, were determined at different volumetric flow rates. It was observed that SHRE increased from 16% to 33% as the volumetric flow rate increased from 85 CFM to 235 CFM in the "cooling mode". Over the same flow range, the Effectiveness was observed to increase from

45% to 60%. Interestingly, there was a steep rise in the performance parameters from 85 CFM to 150 CFM compared to when the volumetric flow rates were increased from 150 CFM to 235 CFM, where a more steady and flatter increase was observed. An error analysis was also conducted to where the standard deviation varied from 0.5 to 3.7% for the SHRE and from 0.2 to 2.3% for the Effectiveness.

Airflow tests and analysis were conducted using the REEL airflow performance testing facility in order to compare the airflow performance data generated in a separate calibrated flow facility, from the newly constructed HRV test facility developed in this study. Initially, it was discovered that the absolute inlet static pressure and absolute outlet static pressure were not similar. In contrast, the supply external static pressure as measured in the REEL testing facility at the HRV's rated 195 CFM was -0.13 inches of water, which was different from the supply external static pressure of 0.4 inches of water obtained in the HVI accredited lab report. This inconsistency in data was attributed to the REEL testing facility's design where there is a large difference in cross-sectional areas between the rectangular duct and circular duct especially near the heating coil, which produces a static pressure loss. In the future, this loss can be offset by introducing a smoother transition between the two different cross-sectional areas. Furthermore, possible leaks can be investigated, while duct lengths might possibly be reduced to alleviate the pressure drop.

Finally, a thermal analysis was conducted at the rated volumetric flow rate. Specifically, the temperature difference between the supply inlet and the supply outlet in the supply side was 6.7°C, while the temperature difference between the exhaust inlet and the exhaust outlet in the exhaust side was 7.9°C at a rated flow of $195 \pm 13\ CFM$. The tolerance was based on the uncertainty of the velocity sensor used. If both flow streams had equal flows, then you would expect similar temperature changes. An additional study was done to determine the relation between T_{supply} and

$T_{exhaust}$ at varying volumetric flow rate. It was observed that the T_{supply} increases, and the $T_{exhaust}$ decreases with a rise in the volumetric flow rate, which could be a result of air leakage between the supply streams and exhaust streams at higher volumetric speeds.

REFERENCES

[1] HOME VENTILATING INSTITUTE, "New Metric Available for HRV and ERV Performance," 2020.
[Online]. Available: https://www.hvi.org/resources/publications/builder-guide/.

[2] HOME VENTILATING INSTITUTE, [Online]. Available: https://hvi-1491.quickbase.com/db/bh6688vwb?a=dr&ifv=1&rid=11754&dfid=12.

[3] A. M. a. C. A. I. Inc, AMCA Standard 210-16 Laboratory Methods of Testing Fans for Certified Aerodynamics Performance Rating, 2016.

[4] ASHRAE, 2017 ASHRAE Handbook -- Fundamentals, Ashrae; Har/Cdr edition , 2017.

[5] ASHRAE, 2020 ASHRAE Handbook—HVAC Systems and Equipment, Addison-Wesley Professional, 2020.

[6] C439-09 Standard laboratory methods of test for rating the performance if heat/energy - recovery ventilators, Canadian Standards Association, 2009.

[7] D. Boyer, "CHOOSING BETWEEN AN HRV AND AN ERV," ECO Home, 18 February 2014. [Online]. Available: https://www.ecohome.net/guides/2276/choosing-between-an-hrv-and-an-erv/.
[Accessed 7 October 2020].